

See discussions, stats, and author profiles for this publication at: <https://www.researchgate.net/publication/324857716>

# X-ray computed tomography study of the flight-adapted tracheal system in the blowfly *Calliphora vicina* analysing the ventilation mechanism and flow-directing valves

Article in *Journal of Experimental Biology* · April 2018

DOI: 10.1242/jeb.176024

CITATIONS

9

READS

148

4 authors, including:



**Lutz Thilo Wasserthal**

Friedrich-Alexander-University of Erlangen-Nürnberg

59 PUBLICATIONS 1,501 CITATIONS

SEE PROFILE



**Rainer H Fink**

Friedrich-Alexander-University of Erlangen-Nürnberg

215 PUBLICATIONS 5,543 CITATIONS

SEE PROFILE



**Lennard K. Wasserthal**

Friedrich-Alexander-University of Erlangen-Nürnberg

6 PUBLICATIONS 34 CITATIONS

SEE PROFILE

Some of the authors of this publication are also working on these related projects:



Interaction of long-tongued hawkmoths and long-spurred flowers and predators [View project](#)



Epitaxial growth of thin organic films on crystalline supports [View project](#)

## RESEARCH ARTICLE

# X-ray computed tomography study of the flight-adapted tracheal system in the blowfly *Calliphora vicina*, analysing the ventilation mechanism and flow-directing valves

Lutz Thilo Wasserthal<sup>1,\*</sup>, Peter Cloetens<sup>2</sup>, Rainer H. Fink<sup>3</sup> and Lennard Knut Wasserthal<sup>4</sup>

## ABSTRACT

Following the discovery of flight motor-driven unidirectional gas exchange with rising  $P_{O_2}$  in the blowfly, X-ray computed tomography (CT) was used to visualize the organization of the tracheal system in the anterior body with emphasis on the arrangement of the pathways for airflow. The fly's head is preferentially supplied by cephalic tracheae originating from the ventral orifice of the mesothoracic spiracle (Sp1). The respiratory airflow during flight is a by-product of cyclic deformations of the thoracic box by the flight muscles. The air sacs below the tergal integument (scutum and scutellum) facilitate the respiratory airflow: the shortening of the thorax turns the scutellum and the wings downward and the scutum upward with a volume increase in the scutal air sacs. The resulting negative pressure sucks air from Sp1 through special tracheae towards the scutal air sacs. The airflow is directed by two valves that open alternately: (1) the hinged filter flaps of the metathoracic spiracles (Sp2) are passively pushed open during the upstroke by the increased tracheal pressure, thereby enabling expiration; (2) a newly described tracheal valve-like septum behind the regular spiracular valve lids of Sp1 opens passively and air is sucked in through Sp1 during the downstroke and prevents expiration by closing during the upstroke. This stabilizes the unidirectional airflow. The tracheal volume of the head, thorax and abdomen and their mass were determined. Despite the different anatomy of birds and flies, the unidirectional airflow reveals a comparable efficiency of the temporal throughput in flies and hummingbirds.

**KEY WORDS:** Tracheae, Spiracles, Auto-ventilation, Synchrotron, X-ray imaging, Micro-tomography, Insect respiration, Gas exchange

## INTRODUCTION

In insects, respiratory gas exchange is provided by the tracheal system, consisting of cuticular branching tubes, guiding the air to the tissues. The blind ends allow only diffusive gas exchange. In many insects, air sacs along the broader branches have a supportive function in gas exchange, facilitating storage of gas and bellow-like ventilation by body movements.

To study the 3D insect tracheal system, earlier research relied on histology, using light and electron microscopy. Cross-sections of flight muscles in rhinoceros beetles showed they comprised 40–50% tracheae (Miller, 1966). To quantify the tracheal volume, these methods were expanded by the stereological point count method, producing quantitative data. Schmitz and Perry (1999) found a tracheal volume of 1.3% of a whole stick insect, excluding the appendages, and calculated the diffusing capacity of the tracheal walls. X-ray-based analyses have been used to visualize the ventilation effect on the tracheal system (Wasserthal et al., 2006; Socha et al., 2007, 2008, 2010). For determination of size-dependent tracheal volume and density, X-ray imaging was applied in different tenebrionid beetles, which revealed size-dependent tracheal volumes from 0.5% to 4.8% (Kaiser et al., 2007). A volumetric study of the tracheal system of the flight muscles in *Drosophila* combined the stereological method with X-ray computed tomography (CT) for analysis of the larger tracheae and confocal microscopy for analysis of the finer intramuscular tracheoles (Harrison et al., 2017). The authors focused on tracheal volume of the adults in response to rising oxygen level during larval rearing. X-ray-based functional analyses have been published on the flight mechanism and role of the steering muscles in blowflies (Walker et al., 2014; Deora et al., 2017). In the present study, the X-ray technique was applied, focusing on the tracheal structures and functions involved in flight motor-driven gas exchange, complementing previous papers (Wasserthal, 2015; Wasserthal and Fröhlich, 2017).

Among insects, blowflies are especially powerful and persistent flyers. Their flight efficiency is based on economic adaptations such as being of light weight. Their high metabolism during flight, which is 100-fold above the resting level (Davis and Fraenkel, 1940), requires efficient gas exchange. During flight, a unidirectional respiratory airflow has been documented with inspiration through the anterior mesothoracic spiracles (Sp1) and expiration through the posterior metathoracic spiracles (Sp2). This unidirectional airflow is generated as a by-product of the thoracic flight movements, enabling a rise in the tracheal  $P_{O_2}$  above resting level during flight (Wasserthal, 2015).

The flight motor is extremely sophisticated, with massive indirect power muscles enclosed in a sclerotized but elastic box (Nachtigall, 1985; Miyan and Ewing, 1985; Ennos, 1987; Walker et al., 2014; Deora et al., 2017). It has previously been discussed whether the deformations of the thorax could ventilate the tracheal system (Weis-Fogh, 1964). Weis-Fogh (1964) regarded the small contractions of the dorso-longitudinal flight muscles (DLMs) as not efficient enough for tracheal volume changes. The DLMs show changes in length of only 1–2% in *Sarcophaga* (Boettiger, 1960) or 2–5% of the strain amplitude in *Drosophila virilis* (Chan and Dickinson, 1996). The corresponding deformation of the thorax and tracheal space is only small.

<sup>1</sup>Department of Biology, University of Erlangen-Nuremberg, Staudtstr. 5, D-91058 Erlangen, Germany. <sup>2</sup>European Synchrotron Radiation Facility, 71, Avenue des Martyrs, F-38043 Grenoble, France. <sup>3</sup>Department of Chemistry and Pharmacy, University of Erlangen-Nuremberg, Egerlandstr. 3, D-91058 Erlangen, Germany. <sup>4</sup>Infoteam, D-91088 Bubenreuth, Germany.

\*Author for correspondence (lutz.thilo.wasserthal@fau.de)

 L.T.W., 0000-0002-3195-0194; P.C., 0000-0002-4129-9091; R.H.F., 0000-0002-6896-4266; L.K.W., 0000-0002-5056-7211

To complicate matters, the thoracic spiracles are protected by filter trichomes, which impede unhindered gas exchange by diffusion alone and require a forced respiratory airflow. It was unclear how the airflow was produced and channelled through the tracheal system and which valve structures were responsible for determining the flow direction. Therefore, in our previous study, the movements and the role of the thoracic spiracular valves were analysed during flight (Wasserthal and Fröhlich, 2017). We demonstrated that the hinged posterior filter flaps of Sp2 are passively pushed open during the upstroke of the wings and closed during the downstroke. Thus, the flaps respond to the expiratory airflow through Sp2. The passive opening of the Sp2 flaps by an assumed pressure increase has already been postulated in a detailed anatomical study of the flies' tracheal system (Faucheux, 1973), but has not been observed to be coordinated with the wing beat cycle. By being closed during the downstroke, which is accompanied by a negative pressure pulse (Wasserthal, 2015), the Sp2 flaps indirectly support exclusive inspiration through Sp1.

It remained unclear how the expiratory airflow was entirely prevented from being discharged through Sp1. The fixed filter trichomes at Sp1 do not hinder the inflow and hence cannot be responsible for blocking the outflow. It was hypothesized that an additional tracheal valve must be involved in the formation of the unidirectional airflow. It has been shown that the movements of the regular inner valve lids of Sp1 and Sp2 are not coordinated with the single wing beat cycles. They regulate the concentration of oxygen, water vapour and CO<sub>2</sub> over longer time spans (Wasserthal and Fröhlich, 2017). During steady flight, they open by less than 5%. Wider opening briefly occurs during forced flight, and during feeding and the accompanying digestive metabolism, running and grooming. The mostly only slightly open valve lids prevent equilibration of the tracheal pressure with the atmosphere and maintain a mean sub-atmospheric tracheal pressure, a precondition for the convective inflow of fresh air and the rise of oxygen concentration during flight (Wasserthal, 2015).

In the present study, in addition to the search for a tracheal valve, the tracheal system of the blowfly was analysed on the basis of 3D X-ray micro-CT to investigate the structures involved in producing the airflow and in determining the flow direction. The compliance and expected volume changes were analysed on the basis of video sequences of the moving contours of the thorax.

## MATERIALS AND METHODS

### Animals

Blowflies (*Calliphora vicina* Robineau-Desvoidy 1830) were obtained and used directly from the field or their F1-offspring larvae were reared on pork liver.

### Recording X-ray micro-CT

X-ray micro-CT of blowflies was carried out at the ESRF synchrotron light source (Grenoble, France), beamline ID19. The flies were immobilized and killed with formaldehyde vapour, 2–3 h prior to exposure to X-rays. Monochromatic synchrotron radiation (15 keV photon energy from a double crystal silicon monochromator) was used. A detector with a pixel size of 7.5 µm and a maximum field of view of 15 mm×15 mm was set 40 mm downstream of the specimen, yielding radiographs containing both absorption and phase information. A total of about 1000 radiographs were recorded while the flies were moved half a turn (0.3 s exposure/radiograph). The volumes were reconstructed with the ESRF software PyHST using the parallel beam filtered back-projection algorithm. They were cropped and stored as 8-bit datasets consisting of approximately 1400 slices

with a size of about 1000×1000 pixels of two females and three males. The final spatial resolution in the images was 12 µm. The datasets were analysed with NIH ImageJ and the volumes rendered using TGS Amira 3.1 (Mercury Computer Systems SA, F-33708 Mérignac) on a G5 Macintosh computer.

### 3D volume rendering

To obtain a complete 3D rendering, e.g. 819 slices in the fly, stacks of a maximum of 300 images were put together. The final slice thickness was 10.4 µm, derived from a 8.54 mm long male torso (Fig. 1). The tomographic data were visualized by segmenting the data using the segmentation tool of Amira, which re-sliced the tomographic stacks along the insect longitudinal axis. Segmentation assigned a label to each pixel of the image describing to which region or material the pixel belonged. The resulting segmentation was stored in a separate data object called label field. For volume calculation, the tissue statistics module took a uniform label field as input and computed statistic quantities automatically, integrating the total voxel number of the labelled densities. The voxel number and the voxel number multiplied by the voxel size (7.5 µm) gave the resulting volume in microlitres.

A clear discrimination between the air-filled spaces of the tracheae and the rest of the body was possible by the different absorbance for X-rays and the resulting high contrast. The tracheal lumen was defined in the label field as the region (material) of lowest density. However, the continuity of the tracheae with the ambient air outside the body produced problems. These openings concerned the open spiracles and sinuses of ablated appendages like distal legs and wing veins of the cropped dataset. These leaks had to be individually closed by adding dense fictive material in each 2D slice of the tomogram stack using the Amira brush tool. Segmentation was the prerequisite for surface model generation and accurate volume measurement.

The isolated tracheal system was reconstructed from the space defined by the empty lumen up to the intima, selected as the area of lowest density. The thoracic box was defined by the manually chosen density of the exoskeleton. This led to the 3D reconstruction relieved from the tissues including the intima, haemolymph and all fluid-containing organs with a much higher density than the air-filled tracheae and the ambient air. For analysis of the interior aspect of the tracheal system, the 3D reconstructions were cut using the cutting or clipping plane tools. The interpretation was 'facilitated' by assigning different colours to the inner and outer surfaces, when applying the 'cut-away' technique.

### Determination of mass and tracheal and body volumes

The relative volume fractions of the tracheal system and of the extra-tracheal rest of the head, thorax and abdomen were calculated using the segmentation tool and the tissue statistics module of Amira software. The mass values were deduced by weighing the flies and then, successively and separately, the head, thorax and abdomen (*N*=6 males and 6 females). The volume was determined by fluid displacement, immersing complete flies and then their head, body and thorax in a calibrated glass cylinder with benzyl benzoate, which rapidly suffused the surface without penetrating the insects (*N*=3 males and 3 females). For volume and mass measurements, male and female flies corresponding to the feeding state of the CT specimens were selected.

### Video recording of the tethered mesonotal sclerites

The flies were mostly tethered at the scutellum and more rarely at the anterior scutum. The choice of the right location at the dorsum for

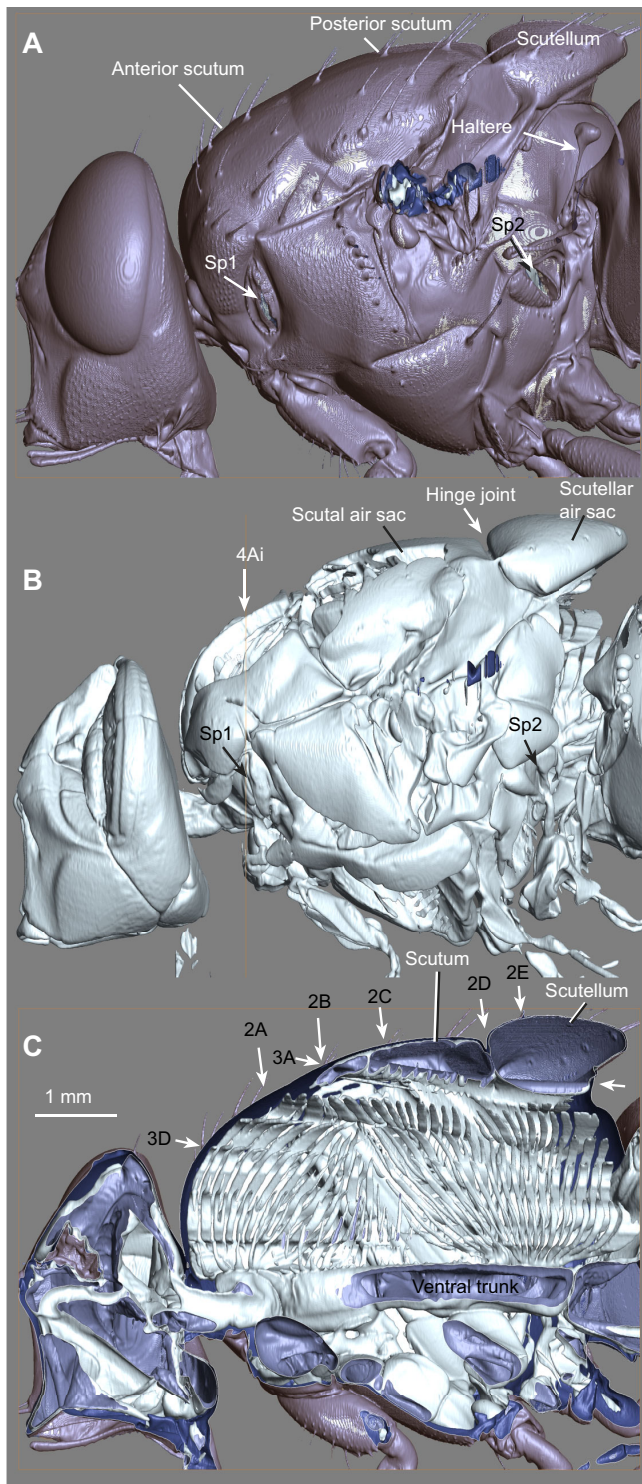


**Fig. 1. Lateral and sagittal X-ray tomographs of the *Calliphora vicina* anterior body.** (A) Left side of the integument. (B) Air sac system directly beneath the integument. (C) Right half of the interior body, showing the tracheae supplying the head, the dorso-longitudinal muscles (DLMs) and the scutal and scutellar air sacs. White, outer tracheal surface; dark blue, inner tracheal surface. Arrows with numbers indicate section planes of Figs 2 and 3 and the slice in Fig. 4Ai.

tethering of the flies was crucial (see Discussion). The elastic glue consisted of thin layers of a 1:1 mixture of Pattex (Henkel, Düsseldorf, Germany) with Fixogum rubber cement (Marabu, Tamm, Germany). Both fixing points had no or little impeding

effect on the mobility of the posterior scutum and scutellum. The teetering movements of the scutal–scutellar complex were visualized using a Sony A9 camera in slow motion mode 100 Hz (1-7-1 Konan Minato-ku, Tokyo, Japan). The posterior border of the scutellum was marked with a pink spot and the top of the posterior scutum was marked with a green spot to clarify the positional changes (Movies 1 and 2).

### Microphotographs of histological sections

As the resolution of the tomographs was only 12  $\mu\text{m}$ , additional histological sections were analysed with regard to the organization of the air sac valve-like septum at Sp1 ( $N=2$ ). The preparation, fixation, embedding and sectioning were performed as described in Wasserthal and Fröhlich (2017), resulting in Toluidine Blue-stained semi-thin sections that were examined with an interference or phase-contrast light microscope (Leitz Ortholux, Wetzlar, Germany).

### RESULTS

The tracheal system of the anterior body of *C. vicina* was analysed using synchrotron X-ray CT and the software Amira. Tomographic cut-away analysis and slices provided an insight into the tracheal system. The 3D reconstructions comprised only the air-filled tracheal spaces inside the boundaries of the tracheal intima. For visualization of the inner tracheal system, the sequential cut-away technique was used after concealing the tissues and the cuticular lining of the exoskeleton (except the integument in Fig. 1A,C).

### The tracheal volume in relation to the mass of the head, thorax and abdomen

Adult flies possess the greatest tracheal volume among insects (in relation to size), but there are no exact quantitative data available. X-ray micro-CT allowed us to measure and calculate the tracheal volumes of the head, thorax and abdomen and to relate these volumes to the corresponding mass and external volume (Table 1). The cephalic tracheal volume was highest in both sexes, accounting for 56% of the head volume in males and 61% in females. The cephalic system consists mainly of large air sacs (Figs 1B and 3A,D). The thoracic volume accounted for 36% in males and 38% in females of the total volume. The 3D volume reconstruction and volumetric calculations may have been somewhat underestimated owing to the spatial resolution of 12  $\mu\text{m}$  of the X-ray tomographs. Those tracheae with a diameter of a few micrometres or tracheoles below 1  $\mu\text{m}$  as in the retina of the eyes or inside the muscle cells are not displayed because of the limited resolution. There was a remarkable difference in the tracheal volume in the abdomen between sexes. The smaller tracheal volume and greater mass of females in contrast to the males (Table 1) were due to the ovaries displacing the pair of abdominal air sacs. In the analysed females, these were almost collapsed in favour of the mature ovaries. A clutch after deposition contained 268 eggs with a mass of 25.75 mg (mean of four females). The volumes of the clutch were 50 and 60  $\mu\text{l}$  ( $N=2$ ). These values were consistent with the calculated sex-specific difference in tracheal volumes.

### Course of respiratory airflow through the tracheal system deduced from anatomy

After passage through Sp1, the inspiratory pathway is split into a ventral (cephalic) and a more dorsal (thoracic) pair of longitudinal trunks, comparable to the primary tracheae of other adult insects (Miller, 1966). The trunks give rise to several air sacs along their course through the thorax and after being connected to the tracheae with de-oxygenated (hypercapnic) air they terminate at Sp2 (Wasserthal, 2015). The discrimination between primary,

**Table 1.** Tracheal volume in different parts of the body in *Calliphora vicina*, calculated from X-ray micro-computed tomography of one male and one female fly and related to mean head and body volumes ( $N=3$  males and 3 females) and mass ( $N=6$  males and 6 females)

	Total volume ( $\mu\text{l}$ )	Mass (mg)		Tracheal volume ( $\mu\text{l}$ )		Tracheal volume (%)		Tracheal volume ( $\text{ml g}^{-1} \text{min}^{-1}$ )	
		Male	Female	Male	Female	Male	Female	Male	Female
Head	18	6	6	10	11	56	61	–	–
Thorax	70	39	41	25	27	36	38	56.0	57.3
Abdomen	30	17	43*	23	3*	77	10*	–	–
Total	118	62	90	58	41			35.08	26.1*

\*Differences in females due to pregnancy.

secondary and tertiary tracheae as used in other insects (Miller, 1966) was not applied to the adult *C. vicina* because there are continuous transitions between the secondary and tertiary tracheae and the intercalated air sacs. The peripheral air sacs form a continuous isolating sheath below the integument displaying the inside surface of the fly's exoskeleton (Figs 1B, 2A,D,E, 3A,D). A dozen cushion-shaped (bulbous-like) air sacs arising from lateral air sacs are stacked laterally and give rise to numerous tracheae penetrating between the fibres of the dorso-longitudinal muscles, termed DLM tracheae (Fig. 2A–C). Between 17 and 34 pairs of these DLM tracheae supplying the six layers of DLM muscles branch and terminate blindly after having demerged (split into) numerous tracheoles inside the muscle fibres. The finest branches and tracheoles were not resolved by micro-CT.

The tracheal supply of the antagonistic dorso-ventral muscles (DVMs) in the lateral thorax is comparable to the arrangement of the DLM tracheae (Fig. 3E). The DLM and DVM tracheae are not simple tubes but are slightly flattened with an oval, rectangular or trapezoid cross-section. This suggests that they can be compressed or dilated depending on the pressure in the haemocoel. Spiral taenidia in these tracheae prevent full collapse. As the orientation between the DLMs and DVMs differs around an angle of 47 deg, the tracheae between the fibres of these antagonistic power muscles are affected differently by the thoracic deformations (Fig. 3E). In a specimen fixed with its wings in the lateral, possibly downstroke position, the DLM tracheae exhibit a wider lumen than the tracheae between the DVM fibres. The lumen of the DVM tracheae looks slit-like. This finding implies a position-dependent opposite autoventilation. The stacks of cushion-shaped air sacs offer a greater volume and compliance than the DLM tracheae, allowing them to function as a bellows system (Fig. 2A–C).

A special feature is the set of approximately 10 pairs of these DLM tracheae in the uppermost storey of the mesonotal muscle layer, which communicate with the paired scutal air sacs. These are caudally connected with the scutellar air sacs. This configuration is crucial for the generation of unidirectional airflow.

#### Connected scutal and scutellar air sacs function as an inflow air pump

Whereas the scutal air sacs are directly connected to the sub-group of 10 pairs of DLM tracheae, the scutellar air sacs, in contrast, are devoid of any direct contact with the DLM tracheae (Fig. 3A–C). They communicate anteriorly with the scutal air sacs and posteriorly with the dorso-ventral air sacs (Figs 2D,E and 3A). Thereby, these scutellar air sacs have broad tracheal connections running ventrally to Sp2, where they meet the primary trunks. As the up and down movements of the scutellum caused by the DLMs and DVMs affect not only the wing beat but also the volume of the air sacs below the scutum, this tracheal arrangement allows better understanding of the respiratory flow path (see Discussion).

#### A tracheal air sac septum behind the mesothoracic spiracle (Sp1) participates in valve function

In the two-dimensional CT slices, the high contrast between the tissue and air-filled spaces allowed visualization of the finest structures, including septal membranes composed of two air sac layers. In serial cross-sections and horizontal sections of the X-ray CT images of the anterior body, a tracheal septum was found on the inner side of the mesothoracic spiracle. This is part of two contacting air sacs, which separate the cephalic tracheal orifice from the thoracic tracheal orifice (Fig. 4A,B). This septum has a free edge, which only incompletely separates the ventral (cephalic) from the dorsal (thoracic) tracheal orifices (Fig. 4Aii,Bii). The structure is corroborated by semi-thin sections (Fig. 5). We conclude that if the pressure increases in the thoracic tracheal system during the wing upstroke, the dorsal air sac inflates and the septum is moved towards the valve lids in the central region of the Sp1 aperture occluding the thoracic tracheal connection (Fig. 6F). The septal edge interacts with the valve lids: if only the middle and ventral part of the valve lids is open, the septal edge occludes the middle part of the aperture, thus blocking expiration from the thoracic tracheae through Sp1. The valve lids of Sp1 are frequently only incompletely open and preferentially only the ventral tracheal orifice is exposed to the ambient air (Fig. 6C).

The thoracic gas exchange is thus partly disconnected from the cephalic system. This mechanism prevents the  $\text{CO}_2$ -loaded (hypercapnic) expiratory gas from being disposed into the cephalic system. This is true during flight with intermediate opening of the Sp1 lids. The preferential fresh air supply for the cephalic tracheal system profits from the expiration blockage of Sp1. The volume of the cephalic tracheal system is relatively large, occupying more than 50% of the total cephalic volume. The mechanisms for cephalic gas exchange are discussed below.

#### DISCUSSION

This study complements previous physiological analyses about flight motor-driven respiratory gas exchange in the blowfly, which appeared as associated papers in Journal of Experimental Biology (Wasserthal, 2015; Wasserthal and Fröhlich, 2017). In *C. vicina*, an efficient  $\text{O}_2$  supply is provided during flight by a unidirectional air flow with inspiration through the mesothoracic spiracles (Sp1) and expiration through the metathoracic spiracles (Sp2). It was hypothesized that the establishment of this directional airflow requires a pressure pump and valves.

It is accepted that the thorax box is deformed by the indirect flight muscles. If the dorso-longitudinal flight muscles (DLMs) contract, they shorten the thorax and raise the mesoscutum, moving the wings downwards (Table 2) (Boettiger, 1960; Nachtigall, 1985; Ennos, 1987; Miyano and Ewing, 1985; Deora et al., 2017). The influence of the bending or buckling of the mesonotum on tracheal pressure in *Schistocerca* has been discussed by Weis-Fogh (1967). He assumed

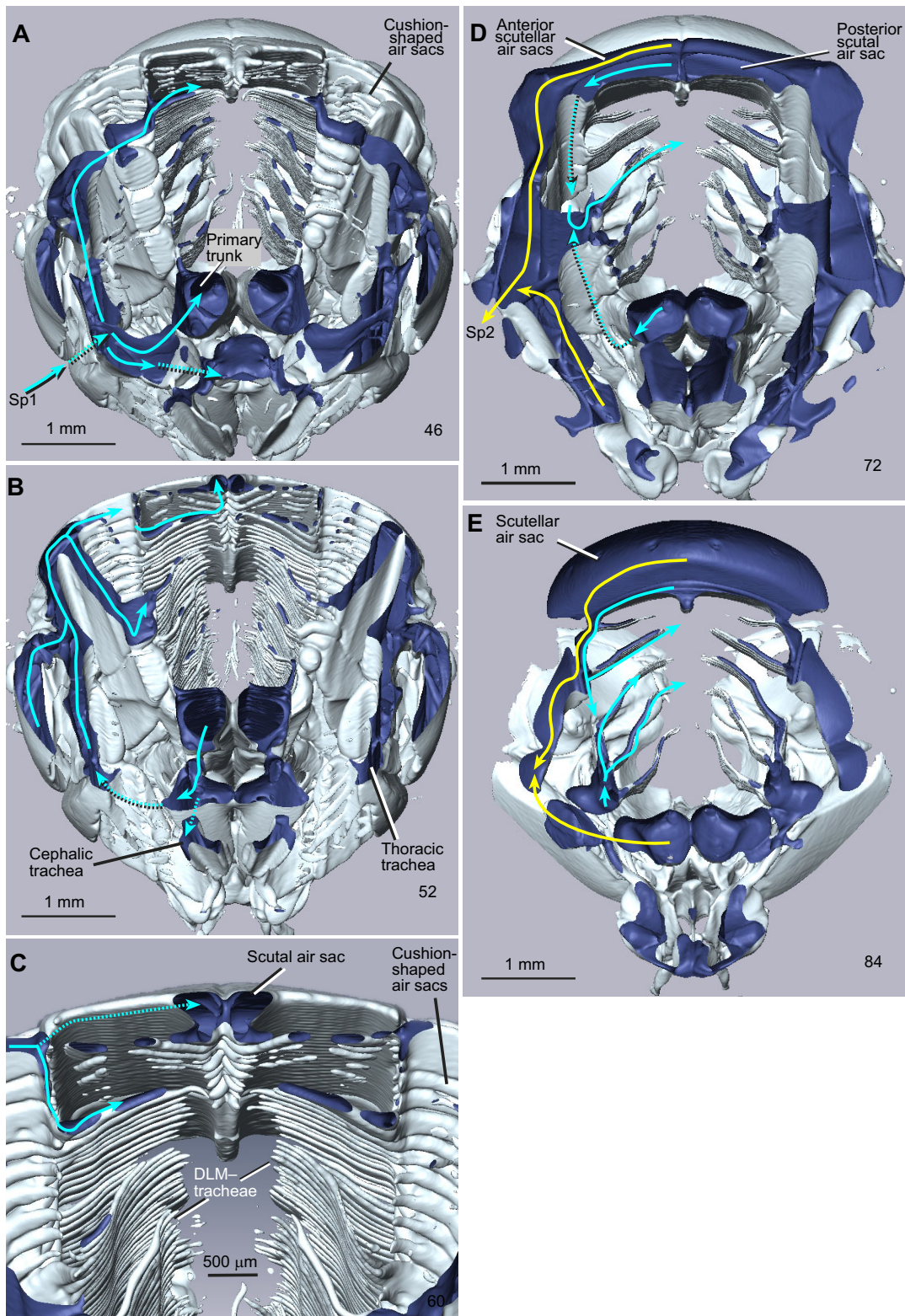


**Fig. 2. Cut-away visualization of the cross-sectioned thoracic tracheal system providing 3D insight caudally into the posterior thorax.**

(A–E) Section planes (numbered bottom right) through the thorax as indicated in Fig. 1. White, outer tracheal surface; dark blue, inner tracheal surface. Blue arrows, deduced inspiratory airflow; yellow arrows, deduced expiratory airflow. (A) Transverse section between the prothorax and mesothorax. The vestibulum behind Sp1 splits into the ventral primary trunks and the dorso- and ventro-lateral thoracic air sacs. (B) Connection of lateral air sacs with stacks of cushion-shaped dorso-lateral air sacs and the tracheae supplying the DLMs. (C) Connection of cushion-shaped air sacs with a series of inter-muscular (DLM) tracheae and scutal air sacs. (D) More posterior section at the border of the mesothorax and the metathorax with the spiracle (Sp2), showing the connection of the scutellar air sacs with the outer lateral air sacs leading to Sp2 and the inner layer of air sacs supplying the tracheae of the posterior DLMs. (E) Metathorax with scutellar air chamber and deduced preferential air flow direction during downstroke (blue arrows) and upstroke (yellow arrows) of the wings.

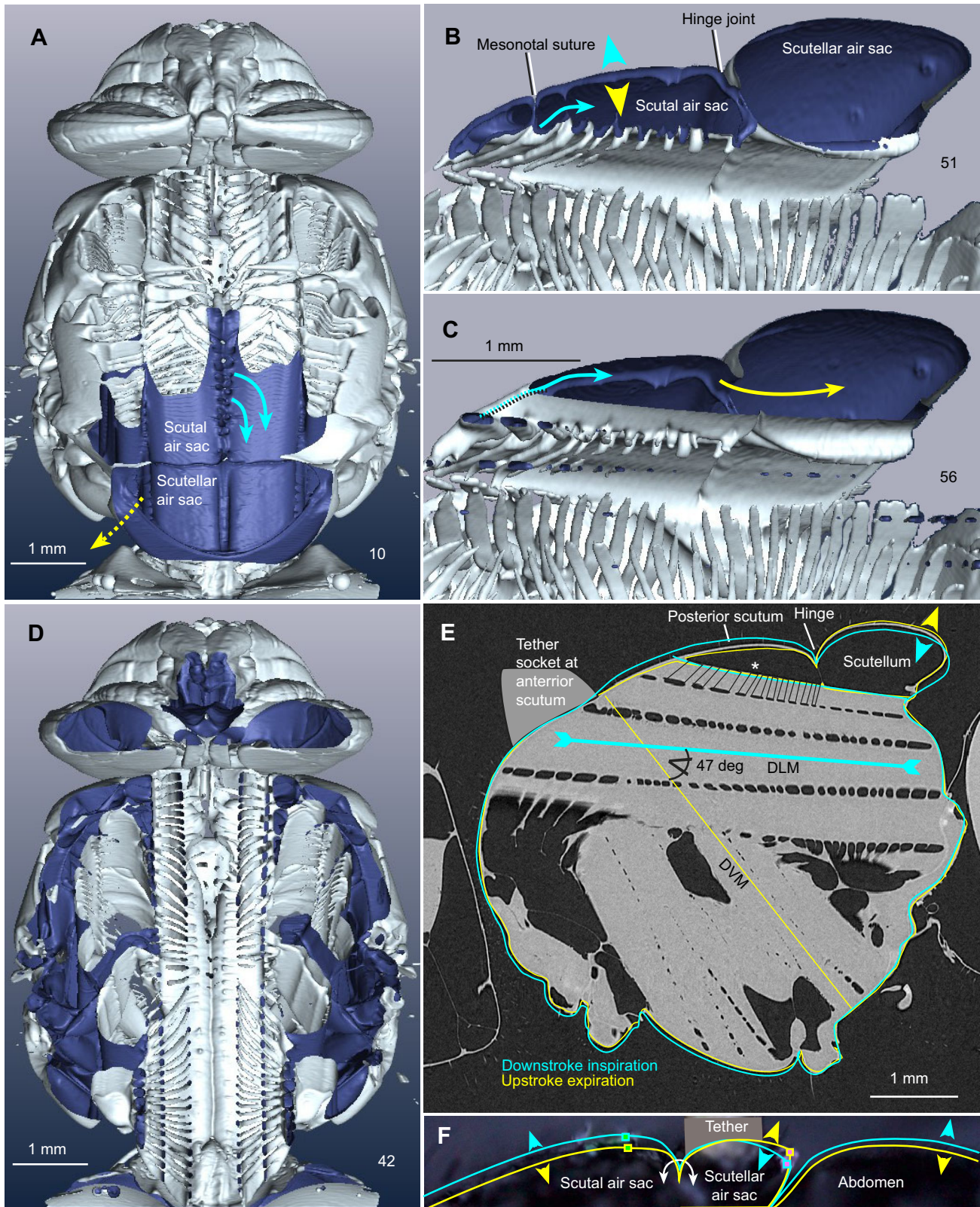


Fig. 3. See next page for legend.

**Fig. 3. Longitudinal sections of the tracheae and air sacs related to cyclic deformations and volume changes during flight.** (A) Cut-away visualization of the horizontal plane exposing the dorsal-most tracheae and air sacs. White, outer tracheal surface; dark blue, inner tracheal surface. While the tracheae open into the scutal air sacs, no such anastomoses occur in the more posterior scutellar air sac. (B) Scutal–scutellar air sac complex ('scutellar pump'). Sagittal plane right of the middle showing the supply of tracheae at the bottom of the scutal air sacs. (C) Cut near the median plane showing the right half of the open connection between scutal and scutellar air sacs. (D) Horizontal view onto the ventral tracheal system after removal of the dorsal half of the body, showing large peripheral air sacs and a central series of tracheae supplying the DLMs. (E) Latero-sagittal section indicating the thoracic deformation during the upstroke and downstroke of the wings. The contours were projected from light video recordings on a computer tomograph. The fly was tethered at the anterior scutum. During the downstroke, the DLMs shorten the thorax and turn the scutellum downwards (blue arrowhead). Asterisk indicates the uppermost level of DLM tracheae. Connection with the scutal air sac added. There was an angle of 47 deg between the DLM and dorso-ventral muscle (DVM). (F) Diagrammatic longitudinal section through the dorsal thorax, from videographic data (Movies 1 and 2). To visualize the small differences in thoracic deformations caused by the downstroke (blue squares and arrowheads) and upstroke (yellow squares and arrowheads) of the wings, the fly was suspended elastically at the scutellum to avoid impediment of the compensatory scutal movements. The most conspicuous change results from up and down movement of the scutellum around the hinged joint by the contraction and relaxation of the dorso-longitudinal flight muscles. The volume of the air sacs below the scutum must increase when the scutellum moves downwards (blue arrowheads). Numbers represent the slice plane.

that in the locust 'this notal ascent could introduce a relatively rapid reduction in tracheal pressure'. He concluded: 'however, this complication does not significantly alter the total amount of ventilation'.

#### The opposite movements of the scutum and scutellum generate a directed airflow, working like an air pump

In the blowfly, the mesonotum does not react uniformly under the deformation of the thoracic box. The scutellum and the scutum perform opposite up and down movements like a teeter. The upward movement of the scutum is caused by the downward bending of the scutellum along the cuticular hinge joint during downstroke of the wings (Fig. 3E,F; Movies 1 and 2).

This scutal lifting during the downstroke has been described in detail in connection with the wing joint (Miyan and Ewing, 1985): 'The parascutal shelf during the downstroke causes a direct lifting of the scutum and DVM II stretch'. In an elaborate study of time-resolved microtomographic imaging of the thorax, blowflies were tethered at the scutum under the supposition that 'the scutum is a stiff, reinforced thoracic structure, and is the standard mounting point for tethered flight preparations in flies' (Walker et al., 2014). These contrary assessments can be explained by the fact that the scutum is a rather long sclerite, which prevents teetering when being tethered at its posterior end or if the scutal–scutellar hinge is filled with glue, but enables teetering when tethered at its anterior scutal end. According to their fig. 10A, Walker et al. (2014) tethered their flies at the anterior scutum, where it had no blocking influence on the mobility of the scutal–scutellar complex.

The moving of the scutum and scutellum affects the pressure and airflow in the air sacs below. If the air sacs below the scutum expand, they must produce a negative pressure pulse (Fig. 7; see figs 2 and 4 in Wasserthal, 2015). The inflow of air is documented by the rising  $O_2$  concentration in the dorsal air sacs. This shows that air is sucked from Sp1 through the 10 pairs of DLM tracheae, which communicate with the scutal air sacs (Fig. 3A–C,F). The suction pressure cannot be equilibrated with the atmosphere via Sp2

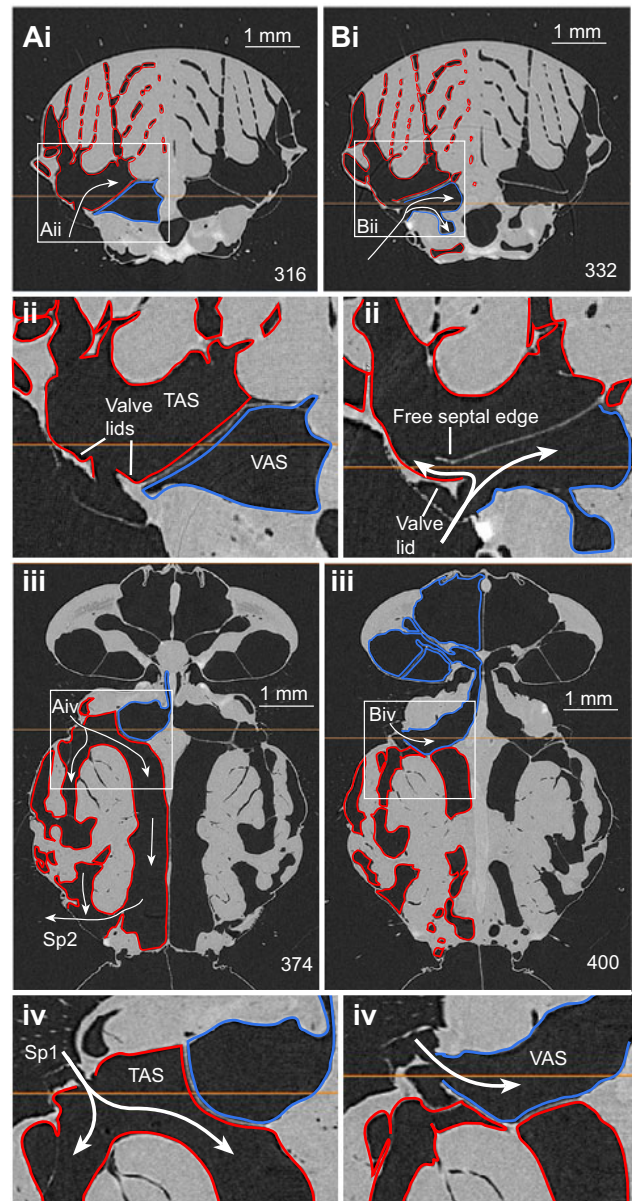


**Fig. 4. Micro-computed tomographs of the anterior body of fixed *C. vicina* at the level of the mesothoracic spiracle, revealing the separate offshoots of the thoracic and the cephalic tracheae.** Grey, tissues; black, air; red contours, thoracic tracheae; blue contours, cephalic tracheae (both of the left side of the body). (Ai, ii) Cross-section at the level of the orifice of the more dorsal thoracic air sac (TAS). (Bi, ii) Cross-section 166  $\mu\text{m}$  more caudal than Ai, at the level of the more ventral spiracular orifice leading into the ventral (cephalic) air sac (VAS) and more dorsal (thoracic) air sac (TAS), showing the free edge of the septal valve in the open (retracted) position, which also allows inflow of air into the thoracic air sac. It is hypothesized that this septum occludes like a backpressure valve, when the pressure rises inside the thoracic tracheae during upstroke of the wings, leaving only the cephalic trachea open as seen in Biv. (Aiii) Horizontal plane showing the flow path (arrows) through the thoracic system, entering at Sp1 and after gathering the de-oxygenated air before leaving at Sp2. (Aiv) Detail of the boxed region in Aiii, showing the open connection of Sp1 to the thoracic trunks. (Biii, iv) Horizontal section, 270  $\mu\text{m}$  more ventral than section Aiii at the level of the orifice facing the ventral (cephalic) air sac (VAS). The more ventral orifice allows air to flow into the cephalic tracheal system. At this level, the thoracic tracheae are separated from the cephalic tracheae. Highlighted orange lines in Aiii and Biii indicate the position of the corresponding cross-sections of Ai and Bi and, reciprocally, lines in Ai and Bi indicate the position of the corresponding horizontal sections in Aiii and Biii. Numbers represent the slice plane.

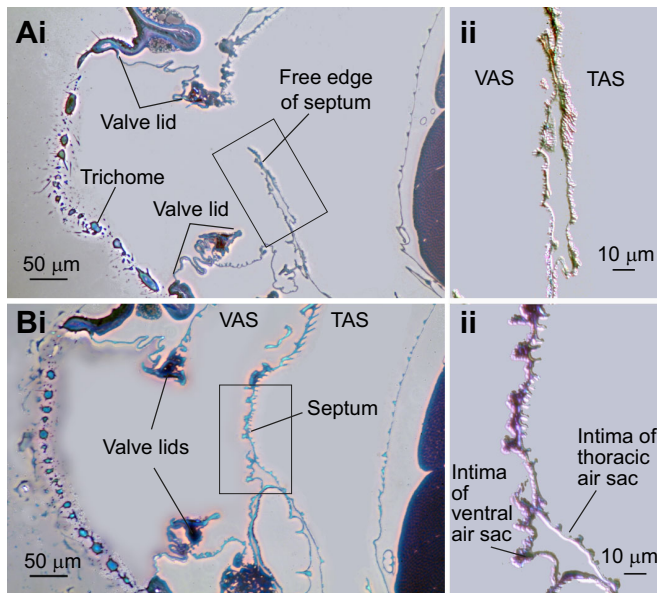


**Fig. 5. Semi-thin horizontal cross-sections through the Sp1 valve in the open condition.** (Ai, Bi) Phase contrast photographs showing the filter trichomes, the valve lids and the air sac septum. (A) The more dorsal section plane with the free upper edge of the septum. (B) The more ventral section plane. (Aii, Bii) Expanded view of interference contrast images (boxed regions in Ai and Bi) with detail of the bilayer septum, which is composed of the intima of the ventral and the thoracic air sacs (VAS and TAS). When the pressure in the thoracic air sacs increases during upstroke of the wings, the septum is assumed to bulge toward the valve lids, thus blocking the aperture between the valve lids and preventing expiratory airflow through Sp1.

because the Sp2 filter flaps close when the tracheal pressure decreases (Wasserthal and Fröhlich, 2017). In this way, they contribute to the unidirectional airflow. When the DLMs relax and the antagonistic DVMs contract, the scutellum moves upwards and the scutum moves downwards (Fig. 3E,F, yellow arrowheads). As the pressure in the scutal air sacs increases, the air is pumped into the scutellar air sacs, from where it is transferred via the lateral air sacs toward Sp2, pushing the filter flaps open. This output direction is ensured because – in contrast to the scutal air sacs – the scutellar air sacs are not connected to the DLM tracheae. A flow-directing effect within the scutal–scutellar air sac configuration is possibly already present independent from the valves, because the resistance against the backflow through the small inflow openings of the scutal DLM tracheae is greater than that against the wider connections of the scutellar air sacs to the dorso-lateral air sacs towards Sp2 (Fig. 2D,E).

The selective influx of this scutellar pump via the 10 pairs of DLM tracheae favours the supply of the dorsal and central DLMs. One may question how the rest of the thoracic tracheal system with more than two dozen blind-ending tracheae between each of the six levels of the DLMs and the seven levels of DVMs is involved in the unidirectional airflow in *C. vicina*. The cyclic deformations probably affect all thoracic tracheae, thus producing a tidal flow. Owing to the valve flaps at Sp2 and the septum valves at Sp1, the tidal flow is prevented from discharging the air through Sp1. Even though the tidal flow may be weak in the blind-ending tracheae between the muscle fibres, the high-frequency small-volume oscillations can presumably enhance the diffusivity of the gases, as has been demonstrated using an experimental vibration frequency of 15 Hz in the lung of beagle dogs (Bohn et al., 1980).

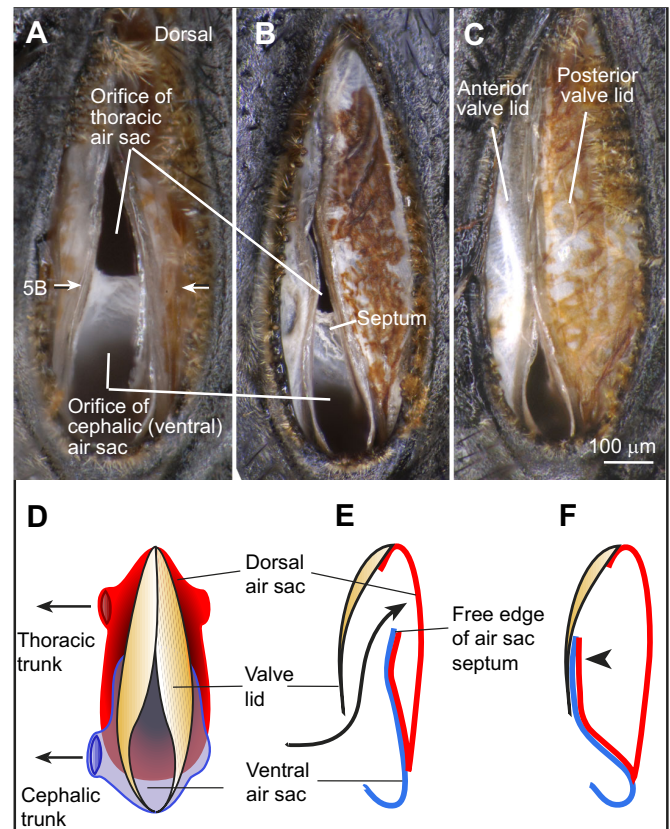


**Fig. 6. Opening conditions of the mesothoracic spiracle and interaction of the valve lids with the air sac septum.** (A–C) Photographs of living Sp1. Filter trichomes were removed to uncover the valve lids and the orifices of the more dorsal (thoracic) and the ventral (cephalic) tracheae. (D–F) Graphs with schematic surface view (D) and longitudinal views of Sp1 (E,F) with different degrees of air sac septum opening and sealing of the thoracic trachea.

(A) Retracted valve lids expose the thoracic and ventral orifice equally after cessation of tethered flight. (B) Situation during 20 s of tethered flight with valve lids reducing the thoracic orifice to a small slit while leaving the ventral part open. (C) Situation during rest. Only the ventral orifice with preferential access to the cephalic trunk is exposed. (D) Valve lids half open, facilitating inspiration via thoracic and cephalic tracheal trunks. (E) With a retracted air sac septum and open valve lids, the orifices of the cephalic trachea (blue) and of the thoracic trachea (red) are open. The free edge of the septum of the thoracic trachea is passively bent inwards by the inflowing air (black arrow). (F) During the increase in pressure in the thoracic tracheae during the upstroke, the air sac septum is moved against the valve lids (arrowhead), screening the cephalic orifice from hypercapnic thoracic air by preventing expiration through Sp1. See also Figs 4Bi,ii and 5. White arrows show the position of the section in Fig. 5B.

**Table 2. Opening and closing of the Sp2 filter flap and Sp1 septum valves correlated with wing beat cycle and up and down movements of the scutum, scutellum, haltere and abdomen**

Wing beat*	Down	Up
DLM	Contract	Relax
Scutellum	Down	Up
Scutum	Up	Down
Haltere*	Up	Down
Abdomen*	Up	Down
Sp1 septum valve	Open	Closed
Sp2 filter flap*	Closed	Open
Thoracic tracheal pressure*	Decrease	Increase
Tracheal air flow*	Sp1 inspiration	Sp2 expiration

DLM, dorso-longitudinal flight muscle. \*Data from Wasserthal (2015).

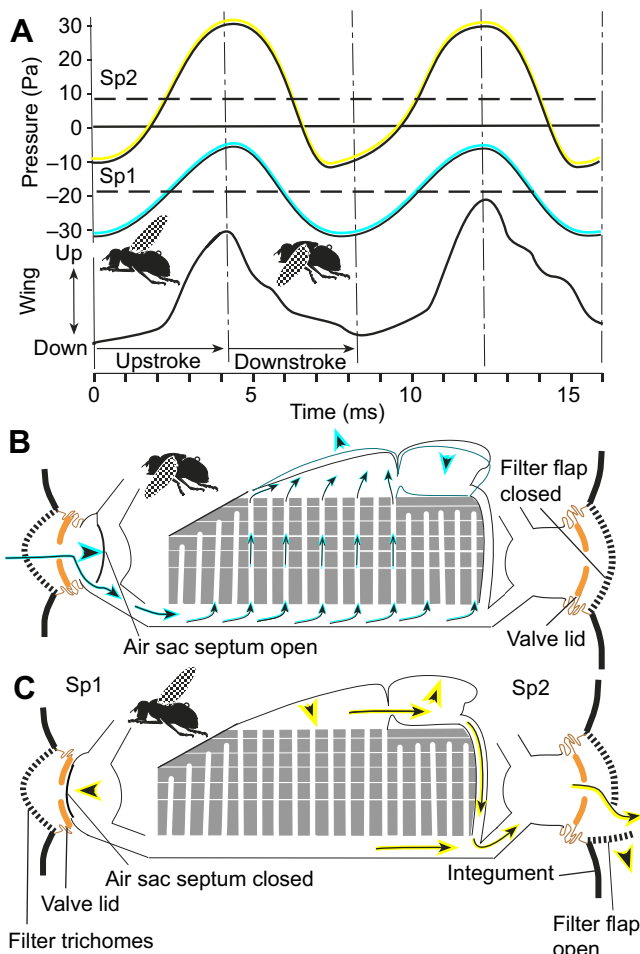


**Fig. 7. Diagram illustrating airflow through the mesothoracic DLM tracheae in response to the volume/pressure changes of the scutal air sacs during the wing beat cycle and the alternating opening and closing of the Sp1 septum valve and Sp2 filter flap.** (A) Tracheal pressure at Sp1 and Sp2 during upstroke and downstroke of the wings correlated with inspiration through Sp1 and expiration through Sp2. From Wasserthal (2015). (B) Inspiration through Sp1 caused by the expansion of the scutal air sacs and suction of air through the tracheae of the DLMs during downstroke of the wings (blue arrows). (C) Expiration during upstroke of the wings. As the tracheal pressure increases, the hinged valve flap of Sp2 is passively pushed open, the air is expired (yellow arrows) and the air sac septum is moved towards the only partly open aperture between the valve lids of Sp1, blocking expiration through Sp1 (arrowheads indicate direction of movement). Orange, slightly open active valve lids.

It is hypothesized that the directed outflow of the scutellar pump and of the other tracheae, which are connected via the lateral dorso-ventral air sacs to the pair of rigid primary longitudinal trunks, is supported by the suction of a jet-pump effect, functioning according to the Bernoulli principle. The septum valves at the tracheal entrance of Sp1 and the flap valves at the exit of Sp2 are situated at strategic locations from where they determine the direction of the entire thoracic respiratory airflow (see below).

The respiratory gas exchange within the finer tracheal branches is suggested to function like a suction-ventilation system, with an inwards direction due to substitution of the consumed oxygen (Buck, 1958; Miller, 1974). The volumetric CO<sub>2</sub> equivalent is buffered and stored in the haemolymph (Bridges and Scheid, 1982; Harrison et al., 1990) and released via larger air sacs and the metathoracic tracheal plexus (Faucheux, 1973; L.T.W., unpublished).

### Valve mechanisms under sub-atmospheric pressure of the tracheal system

As a precondition to holding the air sac lumina open in the adult insect, the haemocoelic pressure remains sub-atmospheric. This sub-atmospheric pressure is established after the post-ecdysial diuresis. Only a thin layer of haemolymph remains surrounding the organs (Wigglesworth, 1963; Nicolson, 1976; Wasserthal, 1996, 1998, 2014). The elasticity of the tracheae and the capillary forces makes them adhere to the inner face of the exoskeleton and to the surfaces of the organs, thus distending the tracheal space and forming an isolating sheath of communicating air sacs mirroring the inner shape of the integument (Fig. 1B). Any deformation of the thoracic box must directly affect the tracheal volume. As the regular spiracular valve lids are mostly only slightly open at rest and even during flight, a basic mean sub-atmospheric pressure is maintained in the tracheal system (Wasserthal, 2012, 2015).

It seemed likely that the regular spiracular valve lids could be responsible for blocking the expiratory airflow through Sp1. However, the regular lids of the Sp1 and Sp2 valves are actively controlled by opener muscles. They cannot be involved in the wing beat-dependent opening cycle, because they are not coordinated with the single wing beat cycles, but regulate the intratracheal pressure and gaseous composition in the range of seconds, not milliseconds (Wasserthal and Fröhlich, 2017).

In *C. vicina*, it can be seen that in the generation of the unidirectional respiratory airflow two other types of valves are involved, which open or close alternately in coordination with the wing beat cycle. The described coordinated movements of the hinged filter flap of Sp2 (see movie 1 of Wasserthal and Fröhlich, 2017) were at first presumed to be sufficient for the formation of unidirectional airflow, but could not explain why no CO<sub>2</sub> was released through the slightly open Sp1. Therefore, an additional mechanism was postulated for tightly blocking the expiration through Sp1 (Wasserthal, 2015). It was suggested that a valve inside the tracheal system should support the unidirectional flow.

To test this hypothesis, an artificial pressure difference in a split chamber experiment was applied in tethered flying *C. vicina*. When increasing the pressure in the insect chamber with the Sp2 and abdominal spiracles – at an excess pressure of only 5 Pa in the insect compartment over the empty chamber with the discharging tubes of Sp1 – blockage of the Sp1 outflow was maintained. However, under un-physiologically high pressure differences over 5 Pa, the flies increasingly refused to fly. With a higher pressure difference of 18 Pa, the airflow could be reversed, leaving at Sp1 (see fig. 9 in Wasserthal, 2015).

These experiments performed to overcome the blockage hint at an intra-tracheal valve that responds to low and small pressure differences, reacting with little inertia but incapable of coping with un-physiologically high pressure. The outflow through Sp1 is thought to be impeded by the described septum on the rear of the Sp1 valve lids. The free edge of this delicate tracheal septum is probably pressed against the valve lids, and closes the central opening in the middle of the lids, when the pressure in the thoracic tracheal system increases slightly during the upstroke of the wings (Figs 5 and 6D–F). Both the Sp1 septum valves and the Sp2 valve flaps react passively on pressure pulses, thus complementing each other (Table 2): whereas during the upstroke, the Sp2 flaps are pushed open, during the downstroke, the Sp1 tracheal septum valves are closed, preventing expiration through Sp1 but allowing inspiration (Figs 6 and 7). Without regulating valves, the pressure changes as a result of the deformations of the thorax would produce a tidal flow with an in- and out-flow at all thoracic spiracles.

The cyclic volume changes affect mainly the thoracic tracheal system. The thorax movements are not known to have a direct mechanical effect on the tracheal system in the head and abdomen in *C. vicina*. Both parts of the body have relatively large tracheal volumes (Table 1). The cephalic system may profit from the inflow during the downstroke via the cephalic trunk of Sp1. But how and when is the CO<sub>2</sub> released from the head as it does not profit directly from the wing beat-supported expiration? The cephalic CO<sub>2</sub> can be transferred via the haemolymph into the posterior body by periodic heartbeat reversals, which occur at a higher frequency during flight (9 min<sup>-1</sup>; Wasserthal, 2015) than during rest (2 min<sup>-1</sup>; Wasserthal, 2014). The periodic volume changes of the cephalic air sacs have been recorded by synchrotron X-ray videographs in resting *Drosophila* (Wasserthal et al., 2006). Additional ventilation effects are produced by the frontal and occipital accessory cephalic pulsatile organs in *C. vicina* (Wasserthal, 1999) and proboscis extension reflexes, which have been recorded by oscillatory CO<sub>2</sub> release patterns in some flying *Drosophila* (Lehmann and Heymann, 2005).

The abdominal air sacs – if not compressed by the mature eggs as in pregnant females – might be ventilated by the up and down movements of the abdomen, which coincide with the cyclic flight muscle movements (Table 2). The transition of the CO<sub>2</sub> from the haemolymph into the abdominal air sacs during flight was deduced from the measured reduction of  $P_{O_2}$  (see fig. 5 in Wasserthal, 2015).

#### High efficiency of gas exchange by high frequent summation of small volumes

The efficiency of the flight motor-driven ventilation in *C. vicina* is indicated by the rise in the  $P_{O_2}$  from 18.6 kPa at rest to 19.5 kPa in the scutellar air sacs of the tethered flying *C. vicina* (Wasserthal, 2015). An increase in muscular  $P_{O_2}$  from rest to flight has also been measured in hawkmoths (Komai, 1998) and bumblebees (Komai, 2001), both occurring within a lower  $P_{O_2}$  range of between 6.27 and 10.10 kPa in the moths and at 6.36±1.83 kPa in bumblebees.

The effectiveness of the unidirectional airflow of the thoracic tracheal system can be deduced from the transported air volume per unit time: the volume of the tracheal system was calculated on the basis of the datasets of the 3D rendering program TGS Amira 3.1. Despite the small amplitude of at least 1% of the thoracic deformation per wing beat cycle, the expiratory airflow is strong enough to push the Sp2 flaps passively open during the upstroke. Measurement of the mean tracheal volume of the thorax in one male and one female *C. vicina* revealed a mean of 26 µl corresponding to 36% and 38%, respectively, of the thoracic volume (Table 1).

The 1% shortening of the DLM would result in an approximately 1% volume compression within the 37% tracheal volume share of the thorax. The tidal volume of 1% thoracic tracheal space is 0.26 µl. But although a 1% change in volume seems very low, the situation is different when one considers the ventilation volume per second, which is obtained by multiplying by the high wing beat frequency of 145 Hz (Wasserthal, 2015). This results in an exchanged air volume of about 0.26×145=37.7 µl s<sup>-1</sup> for a mean thoracic mass of 40 mg, resulting in 2.34 ml min<sup>-1</sup>. For comparison, this equals 56.5 ml g<sup>-1</sup> min<sup>-1</sup> for the ventilation efficiency of the thorax as a mean for both sexes (Table 1). This is a cautious calculation, because this 1% volume change affects only the percentage of compliant tracheal space.

The thoracic ventilation volume must be related to the body mass carried by the flying insect. The total body mass values of the males and gravid females differ due to the developing eggs replacing the space occupied by the abdominal air sacs (Fraenkel, 1935; Evans,

1935). The mean mass of a clutch containing 268 eggs was 25.75 mg, with a volume of 55 µl (N=4). Calculation of the tracheal volume in the male body revealed a value of 58 µl, accounting for 49.15% of the total body volume and a mass of 62 mg. In the female, the tracheal volume was 41 µl, accounting for 34.7% of the total body volume and a mass of 90 mg. A similar sex-specific difference in tracheal body volume has been determined in *Schistocerca americana*, with 40% for males and 7% for females (Lease et al., 2006) using an inert gas volumetric method.

For comparison with other flying animals, the measured data were randomized and standardized in grams and minutes. The ventilation volume was 35.08 ml g<sup>-1</sup> min<sup>-1</sup> in males, and 26.1 ml g<sup>-1</sup> min<sup>-1</sup> in females. Comparison with a hummingbird weighing 6 g and having a ventilation volume of 180 ml min<sup>-1</sup>, which amounts to 30 ml g<sup>-1</sup> min<sup>-1</sup>, reveals that the flies, especially the males, have a ventilation volume within the range of excellent flyers like hummingbirds (Butler, 1991). However, the flies outperform the thoracic ventilation volume of the locust *Schistocerca gregaria*, at 4.16 ml g<sup>-1</sup> min<sup>-1</sup> (Weis-Fogh, 1967), by a factor of 9.

#### Convergent evolution of a unidirectional airflow for efficient gas exchange in insects and birds

The flight motor-driven unidirectional airflow in flies and hawk moths (Wasserthal, 2001, 2015) is reminiscent of the unidirectional airflow through the lung tissue in birds. The vertebrate lung mechanisms evolved from the digestive system restricting inspiration and expiration alternatingly through a single tracheal opening. The birds' inner bronchi and the air sac system are, however, adapted to guide the air unidirectionally through the lung tissues via air capillaries. As no structural valves have been found in birds, it has been hypothesized that the unidirectional flow is due to aerodynamic valving during inspiration and expiration depending on air sac compliance and air flow resistance (Brown et al., 1995; Harvey and Ben-Tal, 2016), also described as 'fluid mechanical valving' (Kuethe, 1988). Birds use additional ventilation muscles moving the sternum with attached flight muscles. Ventilation muscles produce higher pressure pulses than the flight muscles and can be synchronized to coincide with the higher frequent wing strokes in a regular pattern with one of the lower wing beat pressure pulses (1:1 to 1:4; Tucker, 1972; Funk et al., 1992; Schmidt-Nielsen, 1999). In contrast to insects, birds depend on O<sub>2</sub> transport by the blood, which means additional load. This requires an especially large heart in hummingbirds (Schmidt-Nielsen, 1999).

In insects, as in all terrestrial arthropods, the respiratory system evolved from segmental integumental invaginations, independently from the intestine. The thorax segments contain two pairs of large spiracles leading to tracheae with interconnected air sacs supplying the flight muscles. This facilitates the separation of inhalation and exhalation and is the precondition for unidirectional airflow. Without the need for special ventilation muscles other than those in birds, flies and hawkmoths directly use the thoracic deformations by the flight muscles for respiratory gas exchange. In contrast to that of birds, the described insect unidirectional ventilation within the thorax does not depend on special respiration muscles. The insect ventilation mechanism by the flight muscles reveals how the air-filled cuticular tube system for O<sub>2</sub> supply provides the basis for the evolution of flying animals down to a degree of miniaturization not realized in vertebrates.

#### Conclusions

Analysis of the cut-away 3D view into the flies' tracheal system revealed structural details that expand our understanding of the

generation of unidirectional respiratory airflow. Tracing of internal pathways uncovered the specialization of the anterior mesotergal (scutal) air sac for the inflow of fresh air from Sp1 and an outflow of CO<sub>2</sub>-loaded air via the adjoining posterior mesotergal (scutellar) air sac towards Sp2, allowing pumping of air by deformation of the thorax box during alternating flight muscle contractions. The X-ray slices and semi-thin sections revealed the occurrence of an air sac septum at the rear of Sp1, suggesting its role as a back pressure valve, which was postulated on the basis of physiological results (Wasserthal, 2015). The 3D micro-CT technology offers a promising method to analyse and illustrate the extremely diverse tracheal systems of representatives of other arthropods.

#### Acknowledgements

We wish to thank Thomas Messingschlager for constructing the specimen holder and Alfred Schmiedl for support in electronic data processing. We thank Prof. Manfred Frasch, Department of Developmental Biology, University of Erlangen-Nuremberg, for laboratory use. We are indebted to Anja S. Fröhlich for cutting the semi-thin sections. The valuable comments of two reviewers are acknowledged.

#### Competing interests

The authors declare no competing or financial interests.

#### Author contributions

Conceptualization: L.T.W.; Methodology: L.T.W., P.C., L.K.W.; Software: L.K.W.; Validation: L.T.W.; Investigation: L.T.W., L.K.W.; Resources: L.T.W., R.H.F.; Data curation: P.C.; Writing - original draft: L.T.W.; Writing - review & editing: L.T.W.; Visualization: L.T.W., P.C., L.K.W.; Supervision: L.T.W.; Project administration: L.T.W., P.C., R.H.F.; Funding acquisition: L.T.W., R.H.F.

#### Funding

This study was supported by the European Synchrotron Radiation Facility, Project SC-1595.

#### Supplementary information

Supplementary information available online at <http://jeb.biologists.org/lookup/doi/10.1242/jeb.176024.supplemental>

#### References

- Boettiger, E. G.** (1960). Insect flight muscles and their basic physiology. *Annu. Rev. Entomol.* **5**, 1-16.
- Bohn, D. J., Miyasaka, K., Marchak, B. E., Thompson, W. K., Froese, A. B. and Bryan, A. C.** (1980). Ventilation by high-frequency oscillation. *J. Appl. Physiol.* **48**, 710-716.
- Bridges, C. R. and Scheid, P.** (1982). Buffering and CO<sub>2</sub> dissociation of body fluids in the pupa of the silkworm moth, *Hyalophora cecropia*. *Resp. Physiol.* **48**, 183-197.
- Brown, R. E., Kovacs, C. E., Butler, J. P., Wang, N., Lehr, J. and Banzett, R. B.** (1995). The avian lung: is there an aerodynamic expiratory valve? *J. Exp. Biol.* **198**, 2349-2357.
- Buck, J. B.** (1958). Cyclic CO<sub>2</sub> release in insects IV. A theory of mechanism. *Biol. Bull.* **114**, 118-140.
- Butler, J. P.** (1991). Exercise in birds. *J. Exp. Biol.* **160**, 233-262.
- Chan, W. P. and Dickinson, M. H. T.** (1996). In vivo length oscillations of indirect flight muscles in the fruit fly *Drosophila virilis*. *J. Exp. Biol.* **199**, 2767-2774.
- Davis, R. A. and Fraenkel, G.** (1940). The oxygen consumption of flies during flight. *J. Exp. Biol.* **17**, 402-407.
- Deora, T., Gundiah, N. and Sane, S. P.** (2017). Mechanics of the thorax in flies. *J. Exp. Biol.* **220**, 1382-1395.
- Ennos, A. R.** (1987). A comparative study of the flight mechanism of Diptera. *J. Exp. Biol.* **127**, 355-372.
- Evans, A. C.** (1935). Some notes on the biology and physiology of the sheep blowfly, *Lucilia sericata* Meig. *Bull. Ent. Res.* **26**, 115-122.
- Faucheux, M.-J.** (1973). Recherches sur l'appareil respiratoire des diptères adultes. II. *Calliphora erythrocephala* (Cyclorhapha Calliphoridae). *Ann. Soc. Entomol. Fr.* **9**, 413-431.
- Fraenkel, G.** (1935). Observations and experiments on the blow-fly (*Calliphora erythrocephala*) during the first day after emergence. *Proc. Zool. Soc. Lond.* **105**, 893-904.
- Funk, G. D., Steeves, J. D. and Milsom, W. K.** (1992). Coordination of wingbeat and respiration in birds. II. "Fictive" flight. *J. Appl. Physiol.* **73**, 1025-1033.
- Harrison, J. F., Wong, C. J. H. and Phillips, J. E.** (1990). Haemolymph buffering in the locust *Schistocerca gregaria*. *J. Exp. Biol.* **154**, 573-579.
- Harrison, J. F., Waters, J. S., Biddulph, T. A., Kovacevic, A., Klok, C. J. and Socha, J. J.** (2017). Developmental plasticity and stability in the tracheal networks supplying *Drosophila* flight muscle in response to rearing Oxygen level. *J. Insect Physiol.*
- Harvey, E. P. and Ben-Tal, A.** (2016). Robust unidirectional airflow through avian lungs. *PLoS Comput. Biol.* <https://doi.org/10.1371/journal.pcbi.1004637>
- Kaiser, A., Klok, C. J., Socha, J. J., Lee, W.-K., Quinlan, M. C. and Harrison, J. F.** (2007). Increase in tracheal investment with beetle size supports hypothesis of oxygen limitation on insect gigantism. *Proc. Natl. Acad. Sci. USA* **104**, 13198-13203.
- Komai, Y.** (1998). Augmented respiration in a flying insect. *J. Exp. Biol.* **201**, 2359-2366.
- Komai, Y.** (2001). Direct measurement of oxygen partial pressure in a flying bumblebee. *J. Exp. Biol.* **204**, 2999-3007.
- Kuethe, D. O.** (1988). Fluid mechanical valving of air flow in bird lungs. *J. Exp. Biol.* **136**, 1-12.
- Lease, H. M., Wolf, B. O. and Harrison, J. F.** (2006). Intraspecific variation in tracheal volume in the American locust, *Schistocerca americana*, measured by a new inert gas method. *J. Exp. Biol.* **209**, 3476-3483.
- Lehmann, F.-O. and Heymann, N.** (2005). Unconventional mechanisms control cyclic respiratory gas release in flying *Drosophila*. *J. Exp. Biol.* **208**, 3645-3654.
- Miller, P. L.** (1966). The supply of oxygen to the active flight muscles of some large beetles. *J. Exp. Biol.* **45**, 285-304.
- Miller, P. L.** (1974). Respiration-aerial gas transport. In *The Physiology of Insecta*, vol. 6 (ed. M. Rockstein), pp. 345-402. New York: Academic Press.
- Miyai, J. A. and Ewing, A. W.** (1985). How Diptera move their wings: a re-examination of the wing base articulation and muscle systems concerned with flight. *Philos. Trans. R. Soc. Lond. B* **311**, 271-302.
- Nachtigall, W.** (1985). *Calliphora* as a model system for analysing insect flight. In *Comprehensive Insect Physiology, Biochemistry and Pharmacology*, Vol. 5 (ed. G. A. Kerkut and L. I. Gilbert), pp. 501-605. Oxford: Pergamon.
- Nicolson, S. W.** (1976). Diuresis in the cabbage white butterfly, *Pieris brassicae*, fluid secretion by the Malpighian tubules. *J. Insect Physiol.* **22**, 1347-1356.
- Schmidt-Nielsen, K.** (1999). *Animal Physiology*. Heidelberg, Berlin: Spektrum, Akad. Verl., 529 pp.
- Schmitz, A. and Perry, S. F.** (1999). Stereological determination of tracheal volume and diffusing capacity of the tracheal walls in the stick insect *Carausius morosus* (Phasmatodea, Lonchodidae). *Physiol. Biochem. Zool.* **72**, 205-218.
- Socha, J. F., Westneat, M. W., Harrison, J. F., Waters, J. S. and Lee, W.-K.** (2007). Real-time phase contrast X-ray imaging: a new technique for the study of animal form and function. *BMC Biol.* <http://www.biomedcentral.com/1741-7007/5/6>.
- Socha, J. J., Lee, W.-K., Harrison, J. F., Waters, J. S., Fezzaa, K. and Westneat, M. W.** (2008). Correlated patterns of tracheal compression and convective gas exchange in a carabid beetle. *J. Exp. Biol.* **211**, 3409-3420.
- Socha, J. F., Förster, T. D. and Greenlee, K. J.** (2010). Issues of convection in insect respiration: insights from synchrotron X-ray imaging and beyond. *Respir. Physiol. Neurobiol.* **1735**, 565-573.
- Tucker, V. A.** (1972). Respiration during flight in birds. *Respir. Physiol.* **14**, 75-82. [www.com/science/article/pii/0034568772900187](http://www.com/science/article/pii/0034568772900187).
- Walker, S. M., Schwyn, D. A., Mokso, R., Wicklein, M., Müller, T., Doube, M., Stampanoni, M., Krapp, H. G. and Taylor, G. K.** (2014). In vivo time-resolved microtomography reveals the mechanics of the blowfly flight motor. *PLoS Biol.* **12**, e1001823.
- Wasserthal, L. T.** (1996). Interaction of circulation and tracheal ventilation in holometabolous insects. *Adv. Insect Physiol.* **26**, 297-351.
- Wasserthal, L. T.** (1998). The open hemolymph system of holometabola and its relation to the tracheal space. In *Microscopic Anatomy of Invertebrates. Insect Structure*, Vol. 11B/25 (ed. M. Locke and F. W. Harrison), pp. 583-620. Chichester: Wiley-Liss.
- Wasserthal, L. T.** (1999). Functional morphology of the heart and of a new cephalic pulsatile organ in the blowfly *Calliphora vicina* (Diptera: Calliphoridae) and their roles in hemolymph transport and tracheal ventilation. *Int. J. Insect Morphol. Embryol.* **28**, 111-129.
- Wasserthal, L. T.** (2001). Flight-motor-driven respiratory airflow in the hawkmoth *Manduca sexta*. *J. Exp. Biol.* **204**, 2209-2220.
- Wasserthal, L. T.** (2012). Influence of periodic heartbeat reversal and abdominal movements on hemocoelic and tracheal pressure in resting blowflies *Calliphora vicina*. *J. Exp. Biol.* **215**, 362-373.
- Wasserthal, L. T.** (2014). Periodic heartbeat reversals cause cardiogenic inspiration and expiration with coupled spiracle leakage in resting blowflies, *Calliphora vicina*. *J. Exp. Biol.* **217**, 1543-1554.
- Wasserthal, L. T.** (2015). Flight-motor-driven respiratory airflow increases tracheal oxygen to nearly atmospheric level in blowflies (*Calliphora vicina*). *J. Exp. Biol.* **218**, 2201-2210.
- Wasserthal, L. T. and Fröhlich, A. S.** (2017). Structure of the thoracic spiracular valves and their contribution to unidirectional gas exchange in flying blowflies *Calliphora vicina*. *J. Exp. Biol.* **220**, 208-219.
- Wasserthal, L. T., Cloetens, P. and Fink, R.** (2006). Synchrotron X-ray videography and -tomography combined with physiological measurements for analysis of circulation and respiration dynamics in insects (*Drosophila* and

Calliphora). Deutsche Tagung für Forschung mit Synchrotronstrahlung, Neutronen und Ionenstrahlen an Großgeräten, Hamburg, F-V55.

**Weis-Fogh, T.** (1964). Diffusion in insect wing muscle, the most active tissue known. *J. Exp. Biol.* **41**, 229-256.

**Weis-Fogh, T.** (1967). Respiration and tracheal ventilation in locusts and other flying insects. *J. Exp. Biol.* **47**, 561-587.

**Wigglesworth, V. B.** (1963). A further function of the air sacs in some insects. *Nature* **198**, 106.